Research Article

Hussam Aldeen J. Hassan* and Ressol R. Shakir

Ultimate bearing capacity of eccentrically loaded square footing over geogrid-reinforced cohesive soil

https://doi.org/10.1515/jmbm-2022-0035
received April 01, 2022; accepted April 19, 2022

Abstract: Construction of shallow foundations on weak cohesive soils have limited load-bearing capacity and excessive vertical displacement. This may cause structural damage and reduce the structure's durability. Traditionally, weak cohesive soils are excavated and replaced with another stronger material layer, or the foundation is enlarged. These procedures are costly and time-consuming. However, these soils are also difficult to stabilize due to their low permeability and slow consolidation. Therefore, it has become necessary to use geosynthetic material. In this study, a square footing model with an eccentric load was tested in geogrid-reinforced clay. The adopted load eccentricity ratios were 0.05 to 0.1, 0.16, and 0.25. Twenty-one tests were executed to estimate the reinforcement influence and eccentricity on the ultimate bearing capacity (UBC). The geogrid improved the BC by 2.27 and 2.12 times compared to unreinforced soil for centrical and eccentrical loads, respectively. The best first layer ratio and the best number of reinforcements were found to be 0.35 and 4. A new equation for BCR with knowing the number of reinforcing layers was proposed and compared with other studies' outcomes. It was concluded that the foundation tilts in a linear relationship with eccentricity, with a smaller rate inside the core than outside.

Keywords: bearing capacity, settlement, eccentric load, square footing, geogrid, clay soil, tilt

1 Introduction

One of the economic choices in civil engineering to strengthen the ground is by using geosynthetic reinforcing layer(s) [1,2]. The idea is that the reinforcement components contain tensile loads or shear stress in the structure, minimizing shearing or excessive deformation failure [3]. Most industrial application foundations are subjected to moments and vertical forces, causing eccentric loading. Because of these loads, the total stability of the foundation is decreased together with the differential settlement, foundation tilting, and heaving of the underlying soil, which cause a reduction in the bearing capacity (BC) [4]. However, limited studies have been executed to investigate the effects of eccentricity and reinforcing combination on cohesive soil with a square footing, especially in Iraq. El Sawwaf [5] evaluated the strip footing under eccentric pressure laid over a sand soil reinforced with geogrid and observed that at lower e/B, the influence of reinforcement on BCR is greater, reaching 1.7 as a BCR value. Jawad *et al.* [6] improved the sandy soil using a single geogrid layer with a BCR equal to 1.22. Badakhshan and Noorzad [7] observed that the rate of tilt increases as e/B increases. According to Shadmand *et al.* [8], the geocell reinforcement optimum first layer depth ratio $(u/B)_{op}$ is between 0.25 and 0.40. Also, Lingwal and Gupta [9] found that $(u/B)_{op}$ ranged between 0.35 and 0.51. Al-Shamaa *et al.* [10] studied the geocell-reinforced sand and observed an enhancement of BC of 1.65. For more studies and models related to soil reinforcement, especially geogrids [11].

This study aims to improve the BC and reduce the eccentricity ratio (e/B) impact on the weak clay soil by reinforcing it with geogrid layers. This reduces the use of common, costly, and time-consuming methods such as increasing the footing size or replacing the underneath soil and increasing the use of reinforcing materials. Several essential parameters were evaluated and studied to find the best values and compared with other studies' outcomes. The parameters are load eccentricity (e/B), depth of the topmost reinforcement layer (u/B), number of reinforced layers (N), and footing tilt.

* **Corresponding author: Hussam Aldeen J. Hassan,** Civil Engineering Department, University of Thi-Qar, Thi-Qar, Iraq, e-mail: enghussamd@utq.edu.iq
Ressol R. Shakir: Civil Engineering Department, University of Thi-Qar, Thi-Qar, Iraq, e-mail: rrshakir@utq.edu.iq

Table 1: Characteristics of the soil

Properties	Data	Test standard
Specific gravity G.S	2.65	ASTM D854 [13]
Liquid limit L.L%	35	ASTM D4318 [14]
Plastic limit P.L %	20	
Plasticity index PI%	15	
Maximum dry unit weight (kN/m^3)	18.7	ASTM D1557 [15]
Optimum moisture content %	14.8	
Cohesion (kN/m^2)	51	ASTM D6528 [16]
USCS classification	CL	ASTM 422 [17] and ASTM 2487 [18]

2 Materials

In the experimental work, clay soil was used and taken from a soil quarry near the Nasiriyah-Jabaish road in Thi-Qar City, Iraq. The soil has a plasticity index of 15. Then, it is cleaned of debris, grass, and other organic matter. Table 1 shows the characteristics of soil. Figure 1 shows the utilized steel plate square footing model with 22 mm thickness and 90 mm width (B), taking into account that the vertical generated stresses vanish at a distance of 3.5B from the base of the foundation and do not overlap with the base of the box, and the horizontal generated stresses vanish at a distance of 1.5B and do not overlap with the walls of the test box depending on Bossineq's approach [12]. In order to simulate field conditions, a thin covering of sand was pasted onto the footing plate bottom. Circular grooves are opened on the footings to apply loads with varying eccentricities. The foundation eccentricity ratios are 0.05 and 0.1 below the core boundary, 0.16 at the boundary of the footing core, and 0.25 above the boundary of the footing core. The boundary of the footing core is the portion of the footing that experiences compression when the load is applied anywhere but the center. Loading on the boundary of the footing core vanishes the pressure at the edge of the footing. A Polypropylene geogrid was used as a reinforcement, which has the characteristics given in Table 2.

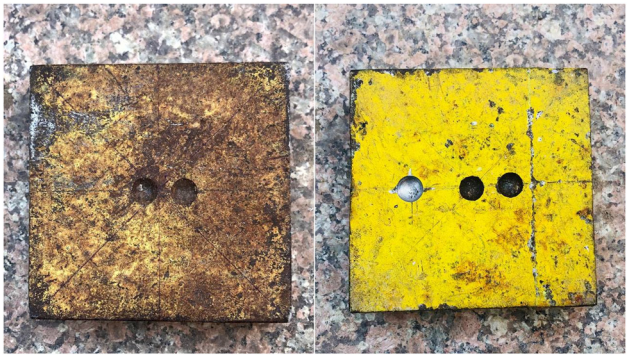

Figure 1: Footing model.

3 Test apparatus and experimental program

This study used a special test device designed in ref. [19] with some tools and accessories, which is shown in Figure 2. Laboratory tests are conducted in a test box measuring 0.60 m in length, 0.60 m in width, and 0.5 m in height. A hydraulic jack powered by electricity is utilized to apply the load. The applied load is measured using two 1,000 and 5,000 kg load cells. The displacements are measured by electronic dial gauges. For unreinforced soil tests, the soil was mixed with the pre-calculated water content. Let the soil soak in the water for a few days. Later, the compaction of soil was done with three 165 mm thick layers in the test box. Different blow numbers were tried and the corresponding density was checked with the core cutter test for each trial until the required density was achieved, which corresponds to the required number of blows. The required number of blows was achieved for every layer to fulfill the energy equivalent of the modified proctor test at 17.88 kN/m^3, which is equal to 95.6% of the maximum dry density for all tests. Using the core cutter method, the density was checked for a few first tests to see how density changes with compaction. This was repeated for each layer to achieve the desired thickness. The final layer is scraped and leveled. The same previous steps are followed for the reinforced soil by adding geogrid layers

Table 2: Geogrid physical and mechanical properties

Characteristics type	Parameter	Data	
Physical characteristics	Structure	Bi-oriented geogrids	
	Type of mesh	Rectangular apertures	
	Standard color	Black	
	Type of polymer	Polypropylene	
Dimensional characteristics	Aperture size (mm)	MD[(a)]	41
		TD[(b)]	34
Technical characteristics	Strength at 0.5% strain (kN/m)	MD	6.5
		TD	7.5
	Strength at 2% strain (kN/m)	MD	16
		TD	17.5

(a) MD: machine direction (longitudinal to roll), (b) TD transverse direction (across roll width).

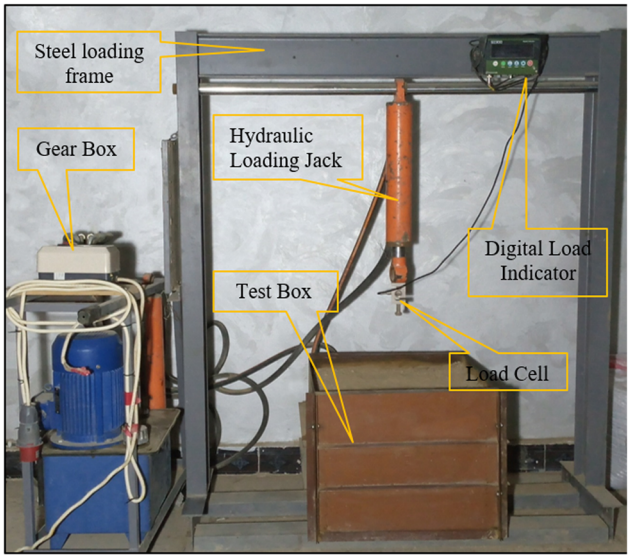

Figure 2: Laboratory test machine [21].

with different u/B and different numbers. Finally, the foundation was placed on the soil. The axial or eccentric load was applied to the footing as specified in ref. [20].

4 Results and discussion

This study will use two terms to assess the benefits of reinforcing the soil. The first term is the bearing capacity ratio (BCR), which is the BC of reinforced soil divided by that of unreinforced [22] as follows:

$$\mathrm{BCR} = \frac{Q_{u\ (\mathrm{reinforced})}}{Q_{u\ (\mathrm{unreinforced})}}, \tag{1}$$

where $Q_{u(\mathrm{reinforced})}$ and $Q_{u(\mathrm{unreinforced})}$ are the UBC of reinforced and unreinforced soil, respectively, Additionally, the definition of reduction factor [23] can be introduced as given below:

$$\mathrm{RF} = \frac{Q_{u(\mathrm{centric})} - Q_{u(\mathrm{eccentric})}}{Q_{u(\mathrm{centric})}}, \tag{2}$$

where $Q_{u\ (\mathrm{centric})}$ and $Q_{u(\mathrm{eccentric})}$ are the UBC of centric loading and eccentric loading, respectively, with both in the same state. The 0.1B method will be used in this study, and all figures have a limit of 25 mm or larger as a maximum tolerated settlement [24]. The 21 experimental tests were executed to assess the stress settlement relationship between the soil and values of UBC for unreinforced and reinforced cases. Table 3 shows the total of 21 tests and their results.

4.1 Effect of first layer depth ratio

The ratio of u/B was evaluated by placing a single layer of geogrid at various u/B to estimate the optimum ratio $(u/B)_{\mathrm{op}}$. Figure 3 shows the pressure-settlement curve for a single geogrid. From Figure 3, the bearing pressure increases with u/B. Figure 4 shows the variation in BCR

Table 3: The geogrid-reinforced clay soil experimental test outcomes

Test no.	Reinforcement	u/B	Eccentricity ratio (e/B)	q (kN/m^2)	RF	BCR
1	None	None	Centric	255	0.00	1.00
2	None	None	$e = 0.05$	220	0.14	1.00
3	None	None	$e = 0.1$	175	0.31	1.00
4	None	None	$e = 0.16$	152	0.40	1.00
5	None	None	$e = 0.25$	95	0.63	1.00
6	$N = 1$	0.25	Centric	277	0.00	1.09
7	$N = 1$	0.35	Centric	307	0.00	1.20
8	$N = 1$	0.45	Centric	285	0.00	1.12
9	$N = 1$	0.55	Centric	280	0.00	1.10
10	$N = 2$	0.35	Centric	365	0.00	1.43
11	$N = 3$	0.35	Centric	465	0.00	1.82
12	$N = 4$	0.35	Centric	580	0.00	2.27
13	$N = 5$	0.35	Centric	600	0.00	2.35
14	$N = 1$	0.35	$e = 0.05$	280	0.09	1.10
15	$N = 1$	0.35	$e = 0.1$	235	0.23	0.92
16	$N = 1$	0.35	$e = 0.16$	200	0.35	0.78
17	$N = 1$	0.35	$e = 0.25$	115	0.63	0.45
18	$N = 4$	0.35	$e = 0.05$	540	0.07	2.12
19	$N = 4$	0.35	$e = 0.1$	502	0.13	1.97
20	$N = 4$	0.35	$e = 0.16$	470	0.19	1.84
21	$N = 4$	0.35	$e = 0.25$	265	0.54	1.04

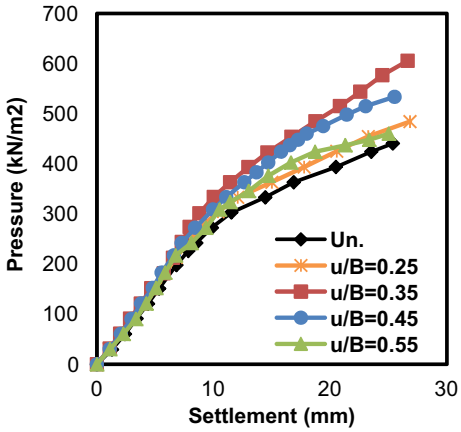

Figure 3: Pressure-settlement curves for different u/B.

with u/B ratios. As may be observed from Figure 4, BCR starts to increase with the increase in u/B values. However, after a certain point, the BCR lowers as u/B increases. Hence, the peak of the curve was obtained as $(u/B)_{op}$ which equals 0.35. This can be attributed to the overburdening at $(u/B)_{op}$ is insufficient to produce frictional resistance at the soil-reinforcement interface, unlike the other values that gave insufficient overburdening. As u/B increases, the BCR decreases and progressively approaches the value of 1.0 because of the depressing of reinforcement [25] or acting as a strong rigid boundary [22,26]. According to Shadmand *et al.* [8], it is noted that $(u/B)_{op}$ falls between 0.25 and 0.40. Sakti and Das [27] suggested that $(u/B)_{op}$ is between 0.35 and 0.4. Lingwal and Gupta [9] concluded that $(u/B)_{op}$ ranged between 0.35 and 0.51.

4.2 Effect of reinforcement layers number (*N*)

Various geogrid layer numbers were used at vertical intervals between consecutive layers (h/B) equal to $(u/B)_{op}$.

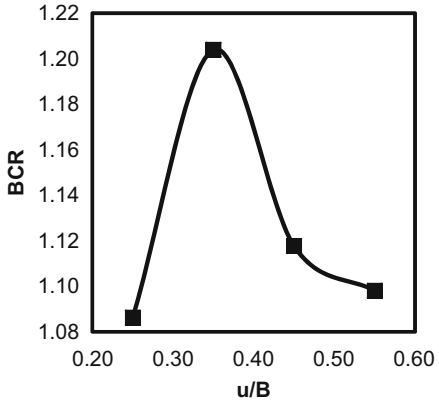

Figure 4: BCR *versus* u/B curve of a single geogrid layer.

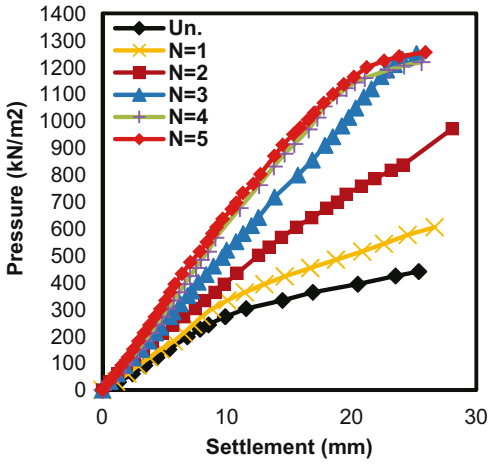

Figure 5: Pressure-settlement curves for different numbers of reinforcements.

Figure 5 depicts the pressure-displacement curves of these experimental tests. As anticipated, the pressure increased as the reinforced layers increased. From Table 3, the increase in BCR was 20, 43, 82, 127, and 135% for 1–5 layers. However, an extra layer has less significance as the number of layers increases. This may be because the reinforcement layers are outside of the foundation influence depth (d/B), which is the overall reinforcement depth below which the BCR increasing rate is negligible. A similar tendency was observed in the studies [28,29]. These results will be discussed in terms of influence depth, which is equal to the optimal number of layers.

Figure 6 shows the BCR variations in different layers and different d/B. From the figure, the BCR increases to 2.27 with a corresponding 4-layer number and 1.4 as d/B. No significant increase in UBC was observed as the d/B value increased. Thus, the optimal d/B is 1.4, which is equivalent to 4 layers. For reinforced clay, Zahraa and Ressol [28],

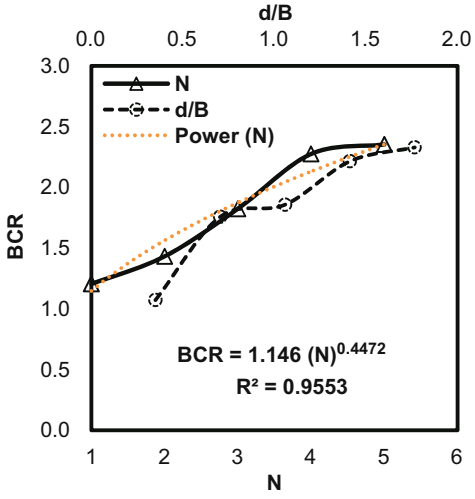

Figure 6: Variation in BCR with *N* and d/B.

Lingwal and Gupta [9], and Chen *et al.* [30] found the ratio of (d/B) of square footing to be 1.25, 1.38, and 1.5, respectively. Boussinesq's solution [31] is utilized to calculate the ratio of pressure increase in the soil to the distributed load on the foundation ($\Delta p/q$, which is equal for this study ($\Delta p/q$ = 0.2) at $d/B \approx$ 1.5 below the center of the foundation, for ref. [30], $\Delta p/q \approx 0.2$ at $d/B \approx$ 1.5 and for ref. [28], $\Delta p/q$ = 0.2 at $d/B \approx$ 1.25. Hence, it appears that the optimum d/B is equal to (1.5), which is approximately equal to the depth at which $\Delta p/q \approx 0.2$.

Based on tests, Figure 6 shows a power equation between N and BCR, which is shown below:

$$\text{BCR} = 1.146(N)^{0.4472}, \quad (3)$$

$$R^2 = 0.9553,$$

where R^2 is the ratio of accuracy and reliability of the equation with the practical results. Eq. (3) has been compared with refs. [9,28], and ref. [30], respectively, in Table 4. The equation showed a fair agreement with the results presented by Zahraa and Ressol [28]. When compared with the results presented by Chen *et al.* [30] and Linqwal and Gupta [9], the equation gives a good agreement when the number of layers is 1 to 3.

4.3 Effect of eccentricity (e/B)

Various eccentricities were utilized. As seen in Figure 7, both unreinforced and reinforced bearing pressure decrease with increase in e/B. It was observed that the corresponding BCR of this reduction increased as e/B increased beyond the core, with the BCR reduction rate of the 4-layer case being 13% for e/B of 0.1–0.16 and 38% for e/B of 0.16–0.25. Sadoglu *et al.* [32] found that the BCR increased in the reinforced case compared to the unreinforced and that this contribution decreases as e/B increases. Badakhshan *et al.* [33] noted that as e/B increases beyond the footing core boundary, the rate of reduction in UBC also increases.

Table 4: Equation *vs* estimated BCR of reinforced soil from other studies

N	Measured BCR	Chen *et al.* [30]		Lingwal and Gupta [9]		Zahraa and Ressol [28]	
		BCR	Error%	BCR	Error%	BCR	Error%
1	1.15	1.2	5	1.27	11	1.24	8
2	1.56	1.27	−19	1.42	−9	1.62	4
3	1.87	1.73	−8	1.6	−15	1.81	−3
4	2.13	1.6	−25	1.62	−24	2	−6

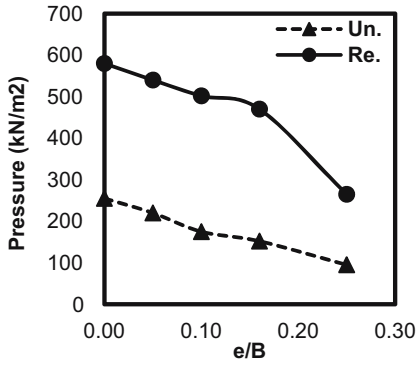

Figure 7: Pressure *vs* e/B curves for reinforced and unreinforced cases.

Also, from Figure 8, the unreinforced curve exhibits larger RF values than the reinforced one, indicating that the unreinforced curve increases more than the reinforced one. Therefore, geogrid reinforcement significantly enhances the UBC of square footing under eccentric load. El Sawwaf [5] indicated a close enhancement in the BCR of reinforced strip footing under eccentric load, where the BCR values at 0.1 e/B are equal to 1.7 for 4 reinforcement layers. The corresponding BCR value in this study was higher by 15% than in ref. [5]. Hence, it is reported that this enhancement may lead to a large reduction in the foundation dimension and the ratio of e/B and thus lead to improved performance and cost-effective design of the foundation.

In Figure 9(a and b), pressure-displacement curves in the unreinforced cases and pressure-displacement curves in the 4-layer reinforced cases are given.

4.4 Effect of tilting angle

Footing tilt is a known phenomenon that occurs when a footing is exposed to eccentric stress. The tilting angle

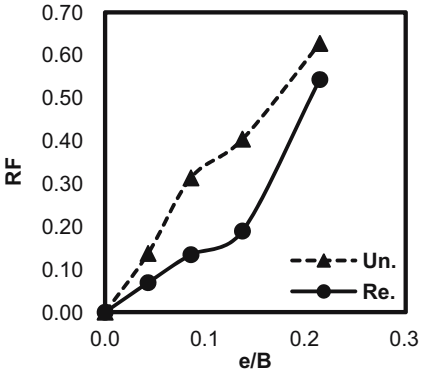

Figure 8: RF *vs* e/B curves for reinforced and unreinforced cases.

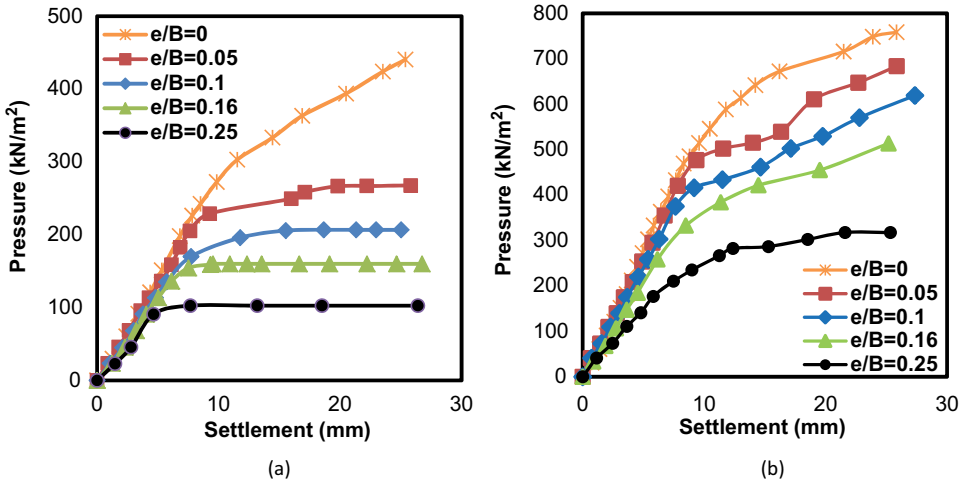

Figure 9: Pressure-settlement curves for various e/B values: (a) unreinforcement soil and (b) reinforced clay with four geogrid layers.

behavior of square footing under the influence of geogrid layers was investigated. In this study, two dial gauges were utilized to measure the settlement of footing and compute the footing tilt. The tilt of the footing is estimated using the difference in footing settlement measured by two dial gauges. For each test with eccentric loads, footing tilt was assessed. Figure 10 depicts the variation in footing tilt with the footing settlement for four layers of reinforcement with $(u/B)_{op}$ for all e/B values. From the curve for reinforced cases that is shown in Figure 10, it is observed that the tilting is linearly increasing with the settlement. Clearly, the square footing tilt angle does not correspond to the failure of the soil beneath it. This means that the tilting angle keeps rising before and after the soil fails.

Footing tilt (in degree) *vs* e/B for both unreinforced and four-layer reinforced situations is introduced in Figure 11. As predicted, Figure 11 shows that the increase in e/B causes higher tilting angles for the constant reinforced situation. Also, it is observed that the tilt increases linearly with (e/B). Increasing from 0 to 4 in the geogrid layer causes the tilting angle to increase by 2, 6, 18, and 34% for 0.05, 0.1, 0.16, and 0.25 load eccentricities, respectively.

Two tilts with e/B equations are proposed in Figure 11, which is shown below:

$$\text{Tilt} = 97.429\left(\frac{\text{e}}{\text{B}}\right)^{1.3186} \text{ for unreinforced soil,} \quad (4)$$

$$\text{Tilt} = 49.36\left(\frac{e}{B}\right)^{1.079} \text{ for reinforced soil,} \quad (5)$$

where R^2 for the above equations is 0.999 and 0.9968, respectively. From Figure 11, in both unreinforced and

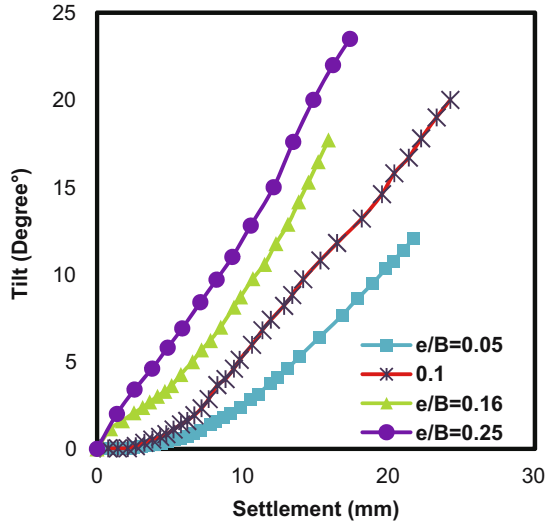

Figure 10: Tilt-settlement curves for four-layer reinforced cases.

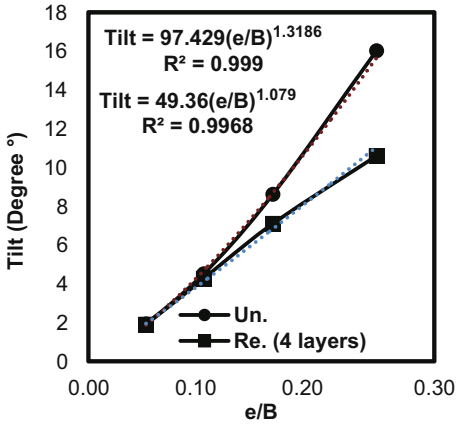

Figure 11: Tilt *vs* e/B for reinforced and unreinforced cases.

reinforced situations, the rate of tilt increment was larger when e/B was outside the core boundary of the footing by 16% than when it was inside the core boundary. As a result, it is concluded that utilizing the reinforcement sheets reduced the tilts of footing as compared to the unreinforced tests, and this decrease increased with larger e/B. This studies' outcomes are slightly close to Badakhshan *et al.* [33] results in tilting.

5 Conclusion

The current research reported results from laboratory tests performed on a square footing with a width of 90 mm sitting on reinforced clay soil under central and eccentrical loadings. According to the findings, the following main conclusions were reached:

1. The best reinforcement layout that gives the best UBC has been observed as 0.35 for (u/B) and 1.4 for (d/B).
2. The number of reinforcements plays an important role in UBC enhancing and reducing settlement until a certain value for geogrid, where the optimum value was 4 with 2.27 BCR.
3. The increase in load eccentricity leads to a reduction in BCR and this reduction is 44% higher when the e/B is beyond the boundary of the footing core.
4. Square footing with more eccentricity has a lower BC regardless of the reinforcing condition. However, this lowering in the reinforced condition is smaller than in the unreinforced one.
5. Soil reinforcing significantly enhances the UBC square foundation under eccentric load, causing a large reduction in the foundation dimension and the ratio of e/B and thus improving the performance and cost-effective design of the foundation.
6. The contribution of increasing UBC using reinforcement as compared to unreinforced situations was decreased with an increase in e/B.
7. The angle of tilt of the footing increases linearly with e/B, and this increasing rate was 16% lower when e/B was inside the core boundary than when it was outside the core boundary.
8. A new equation that relates the BCR to the existing reinforcing layer number was suggested and compared with other studies' findings.
9. Two formulas for calculating the tilt angle of the reinforced and unreinforced clay soil, respectively, were developed under eccentric loading.

Funding information: The authors state no funding involved.

Author contributions: All authors have accepted responsibility for the entire content of this manuscript and approved its submission.

Conflict of interest: The authors state no conflict of interest.

References

[1] Buragadda V, Thyagaraj T. Bearing capacity of jute geotextile-reinforced sand bed. Int J Geosynth Ground Eng. 2019;5(4):1–14.
[2] Nareeman BJ, Fattah MY. Effect of soil reinforcement on shear strength and settlement of cohesive-frictional soil. Int J Geomate Geotech Constr Mater Environ. 2012;3:308–13.
[3] Patel A. Geotechnical investigations and improvement of ground conditions. 1st ed. Sawston, Cambridge: Woodhead Publishing Series in Civil and Structural Engineering; 2019.
[4] Patra C, Behara R, Sivakugan N, Das B. Ultimate bearing capacity of shallow strip foundation under eccentrically inclined load, part II. Int J Geotech Eng. 2012;6(4):507–14.
[5] El Sawwaf M. Experimental and numerical study of eccentrically loaded strip footings resting on reinforced sand. J Geotech Geoenviron Eng. 2009;135(10):1509–18.
[6] Al-Mosawe MJ, Al-Saidi AA, Jawad W, Bearing F. Capacity of square footing on geogrid-reinforced loose sand to resist eccentric load. J Eng. 2015;16(2):4990–9.
[7] Badakhshan E, Noorzad A. Load eccentricity effects on behavior of circular footings reinforced with geogrid sheets. J Rock Mech Geotech Eng. 2015;7(6):691–9.
[8] Shadmand A, Ghazavi M, Ganjian N. Load-settlement characteristics of large-scale square footing on sand reinforced with opening geocell reinforcement. Geotext Geomembr. 2018;46(3):319–26.
[9] Lingwal P, Gupta AK. Bearing capacity of clayey soil reinforced with geogrid. Lecture Notes Civ Eng. 2020;55:173–83.
[10] AL-Shamaa MF, Sheikha AA, Karkush MO, Jabbar MS, Al-Rumaithi AA. Numerical modeling of honeycombed geocell reinforced soil. Lecture Notes Civ Eng. 2020;253–63.
[11] Zahraa Z, Ressol RR. Behavior of foundation rested on geogrid-reinforced soil: A Review. IOP Conf Ser: Mater Sci Eng. 2021;1094:012110.
[12] Bowles JE. Foundation analysis and design. 5th ed. New York: McGraw-Hill; 1997.
[13] ASTM D854. Standard test methods for specific gravity of soil solids by water pycnometer. West Conshohocken, PA: ASTM; 2000.
[14] ASTM D4318. Standard test methods for liquid limit, plastic limit, and plasticity index of soils. West Conshohocken, PA: ASTM; 2005.
[15] ASTM D1557–12. Standard test methods for laboratory compaction characteristics of soil using modified effort (56,000 ft-lbf/ft^3(2,700 kN-m/m^3)). West Conshohocken, PA: ASTM; 2012.
[16] ASTM D6528–17. Standard test method for consolidated undrained direct simple shear testing of cohesive soils. West Conshohocken, PA: ASTM; 2017.

[17] ASTM D422–63. Standard test method for particle – Size analysis soils. West Conshohocken, PA: ASTM; 2002.
[18] ASTM 2487. Standard practice for classification of soils for engineering purposes (Unified Soil Classification System). West Conshohocken, PA: ASTM; 2006.
[19] Altaweel AA, Shakir RR. Analytical model for bearing capacity of two closely spaced foundations. Journal of Physics: Conference Series. Vol. 1973. Issue 1; 2021. p. 012199.
[20] ASTM D1196–93. Method of test for nonrepetitive static plate load test of soils and flexible pavement components for use in evaluation and design of airport and highway pavements. West Conshohocken, PA: ASTM; 2004.
[21] Altaweel AA, Shakir RR. The effect of interference of shallow foundation on settlement of clay soil. IOP Conf Ser: Mater Sci Eng. 2021;1094(1):012043.
[22] Binquet J, Lee KL. Bearing capacity tests on reinforced earth slabs. ASCE J Geotech Eng Div. 1975;101(12):1241–55.
[23] Purkayastha RD, Char RAN. Stability analysis for eccentrically loaded footings. J Geotech Eng Div. 1977;103:647–51.
[24] Herndon RL. Settlement analysis – distribution restriction statement. Department of the Army U.S. Army Corps Eng Wash. 1990;1110:205.
[25] Akinmusuru JO, Akinbolade JA. Stability of loaded footings on reinforced soil. J Geotech Eng Div. 1981;107(6):819–27.
[26] Mandal JN, Sah HS. Bearing capacity tests on geogrid-reinforced clay. Geotext Geomembr. 1992;11(3):327–33.
[27] Sakti JP, Das BM. Model tests for strip foundation on clay reinforced with Geotextile Layers. Transport Res Rec. 1987;1153:40–5.
[28] Zahraa Z, Ressol RR. Bearing capacity of shallow foundation on geogrid reinforced soil. The 4th International Conference on Materials Engineering and Science; 2021 Oct 6–7; Duhok, Iraq. Forthcoming 2021.
[29] Abu-Farsakh M, Chen Q, Sharma R. An experimental evaluation of the behavior of footings on geosynthetic-reinforced sand. Soils Found. 2013;53(2):335–48.
[30] Chen Q, Abu-Farsakh MY, Sharma R, Zhang X. Laboratory investigation of behavior of foundations on geosynthetic-reinforced clayey soil. Transport Res Rec. 2007;2004(1):28–38.
[31] Das BM. Principles of foundation engineering. 8th ed. Boston MA: Cengage; 2016.
[32] Sadoglu E, Cure E, Moroglu B, Uzuner BA. Ultimate loads for eccentrically loaded model shallow strip footings on geotextile-reinforced sand. Geotext Geomembr. 2009;27(3):176–82.
[33] Badakhshan E, Noorzad A, Zameni S. Eccentrical behavior of square and circular footings resting on geogrid-reinforced sand. Int J Geotech Eng. 2018;14(2):151–61.